

Article

Friction and Wear of Hard Yet Tough TiN Coatings Deposited Using High-Power Impulse Magnetron Sputtering

Qian Zhou ^{1,2}, Yixiang Ou ^{1,*} , Feiqiang Li ^{3,*} , Changyu Ou ⁴, Wenbin Xue ², Bin Liao ², Qingsong Hua ^{2,*}, Yunfei Xu ³, Jidong Cao ³ and Guanshu Qu ³

¹ Radiation Technology Institute, Beijing Academy of Science and Technology, Beijing 100875, China; 13622183130@163.com

² Key Laboratory of Beam Technology of Ministry of Education, College of Nuclear Science and Technology, Beijing Normal University, Beijing 100875, China; xuewb@bnu.edu.cn (W.X.); 202031220021@mail.bnu.edu.cn (B.L.)

³ Beijing SinoHytec Co., Ltd., Beijing 100192, China; xuyunfei@autoht.com (Y.X.); caojidong@autoht.com (J.C.); quguanshu@autoht.com (G.Q.)

⁴ School of Environmental and Materials Engineering, Yantai University, Yantai 264005, China; ouchanyu@gmail.com

* Correspondence: ouyx16@tsinghua.org.cn (Y.O.); lifeiqiang@autoht.com (F.L.); q.hua@bnu.edu.cn (Q.H.)

Abstract: The friction and wear response of hard coatings is complex, which largely depends on a good combination of hardness and toughness, and their service life is difficult to predict. Hence, in this work, hard yet tough TiN coatings were deposited using high-power impulse magnetron sputtering at 5–10 kW. With increasing sputtering power, the coatings showed a transition in crystal texture from (200) to (111), along with a refinement in microstructure, leading to an improvement in hardness (H) of 29.8–31.2 GPa and an effective Young's modulus (E*) of 310–365 GPa. The hard yet tough TiN coatings deposited at 6.5 kW exhibited the highest H/E* and H³/E*² ratios of 0.097 and 0.29, respectively, as well as the highest fracture toughness of 2.1 MPa·m^{1/2} and elastic recovery of 42.5%. Accordingly, the coatings possessed an enhanced adhesion and cohesion, in terms of micro-scratch critical load (L_{C3} = 19.67 N) and HF Rockwell HF1 level. The friction and wear response of hard yet tough TiN coatings under the normal load of 1–10 N were investigated to explore their durability and predict their critical load up to failure. Wear mechanisms changed from oxidative to severe abrasive wear, with load increasing from 1 to 10 N. At 2–5 N, a combination of oxidative and abrasive wear was observed. The coatings maintained their integrity up to the critical load of 9.4 N before failure event, with a maximum wear track depth of 1.8 μm, indicating their durability under the loading conditions.

Keywords: hard yet tough; TiN coatings; high-power impulse magnetron sputtering; wear response



Citation: Zhou, Q.; Ou, Y.; Li, F.; Ou, C.; Xue, W.; Liao, B.; Hua, Q.; Xu, Y.; Cao, J.; Qu, G. Friction and Wear of Hard Yet Tough TiN Coatings Deposited Using High-Power Impulse Magnetron Sputtering. *Coatings* **2024**, *14*, 598. <https://doi.org/10.3390/coatings14050598>

Academic Editor: Philipp Vladimirovich Kiryukhantsev-Korneev

Received: 8 April 2024

Revised: 28 April 2024

Accepted: 7 May 2024

Published: 10 May 2024



Copyright: © 2024 by the authors. Licensee MDPI, Basel, Switzerland. This article is an open access article distributed under the terms and conditions of the Creative Commons Attribution (CC BY) license (<https://creativecommons.org/licenses/by/4.0/>).

1. Introduction

As the first-generation of hard ceramic coatings, TiN coatings still show a unique performance in terms of high hardness, good wear, and corrosion resistance, especially for the advancing coating preparation technologies [1–4]. Based on the special needs of different fields, the optimized thickness, density, and microstructure of TiN coatings are deposited on a variety of substrates, to enhance their performance and lifetime, such as cutting tools, mechanical components, and the metal bipolar plates used in hydrogen fuel cells [3,5]. As usual, hard coatings are prone to brittle failure and a lower durability, whereas toughened coatings often compromise on strength. Hard yet tough coatings possess both good hardness and toughness, which exhibits an excellent performance in complex working conditions [6]. It is reported that TiN-based and CrN-based coatings are synthesized as hard yet tough or superhard yet tough coatings by precisely controlling chemical composition and microstructure [7]. TiN coatings, in particular, maintain a broad

phase stability under sufficient nitrogen conditions, offering a versatile range of hardness and toughness [8,9].

The friction and wear response of hard coatings is complex and their failure events are always hard to predict. Thus, it is highly expected that crack initiation and propagation are reduced in hard yet tough coatings, via unique nanostructure mechanisms [10]. In addition, coatings with high hardness and toughness would be beneficial for mild oxidation wear, because of oxide lubricants forming on the sliding contact surface [11]. Finally, the increased thickness of coatings would have a higher bearing capacity during the friction and wear process [6]. Hard yet tough CrN/Si₃N₄ multilayer coatings showed only mild oxidation wear and high cracking resistance during friction measurements, thanks to the block of well-defined CrN/Si₃N₄ interfaces to crack propagation [12]. The tribological behaviors of hard coatings have close relationship with hardness, fracture toughness, and scratch adhesion [13–15]. Zhang et al. [16] reported that hard coatings with good coordination between strength and toughness presented excellent scratch toughness, characterized by critical loads of adhesion failure events in micro-scratch tests. Philippon et al. [17] found that coefficients of friction, wear rates, and endurances were correlated with the mechanical properties, residual stress, and adhesion of the coatings. The improvement in toughness and cohesion/adhesion related to critical loads, L_{C3} , strongly influenced by compressive residual stress promoted a reduction in crack initiation and propagation, as well as oxidative wear during dry sliding tests [4].

The endurance of hard yet tough coatings is affected by the loads applied, mechanical properties, residual stress, etc., resulting in a complex wear response. In this work, TiN coatings were deposited using high-power impulse magnetron sputtering (HiPIMS) at an average target power of 5–10 kW. The effect of the average target power on microstructure, residual stress, mechanical properties, and adhesion were investigated in detail. Moreover, wear responses were further studied to explore the endurance and related mechanisms of coatings at 6.5 kW.

2. Experimental Procedures

2.1. Coating Depositions

The high-power pulse magnetron sputtering technique is a coating preparation method that utilizes high-energy pulse voltages to excite inert gas, creating a plasma that accelerates ions to impact the target material surface, causing sputtering. The high-energy sputtered atoms or molecules deposit on the substrate surface, forming dense, uniform thin films. This method is used to produce high-quality thin films with special functionalities. TiN coatings were deposited on AISI 304 austenite stainless steel substrates using a commercial high-power impulse magnetron sputtering (HiPIMS, Huettinger, Highpulse 4001 G2, Ditzingen, Germany) supply, by sputtering the Ti cylindrical target in an Ar/N₂ mixture gas at a power of 5–10 kW. During the deposition process, the flow rate of Ar gas was 120 sccm and the negative bias voltage was –60 V. The steel substrates (3 mm × 20 mm × 20 mm) were polished with SiC sandpaper up to 5000#, followed by mirror polishing with 0.5 μm micron diamond polishing paste to achieve a surface roughness of 8–10 nm. Before deposition, the substrates were cleaned using denatured acetone and an ultrasonic ethanol bath for 15 min each, followed by drying with N₂ gas. In order to remove the surface contaminants, the substrates were subjected to a two-step etching process consisting of a 15 min Ar gas ion etching with a duty cycle of 4% and a 5 min HiPIMS etching at 2 kW and 6 kW. The Ti layer was deposited on substrates for 5 min at 5 kW and a –60 substrate bias in an Ar atmosphere, in order to enhance the bonding force. The typical process parameters are shown in Table 1. The substrates were mounted in the chamber at a distance of 100 mm from the cylindrical target. The schematic diagram of HiPIMS and the pulse shapes of the target current and voltage during the deposition process are shown in Figure 1.

Table 1. Typical process parameters in the coating deposition process.

Cathode Sources	Substrate Bias (V)	Duty Ration	Frequency (Hz)	Power (kW)	Pulse (μ s)
Pure Ti target	-60	40%	100	5/6.5/8/10	30

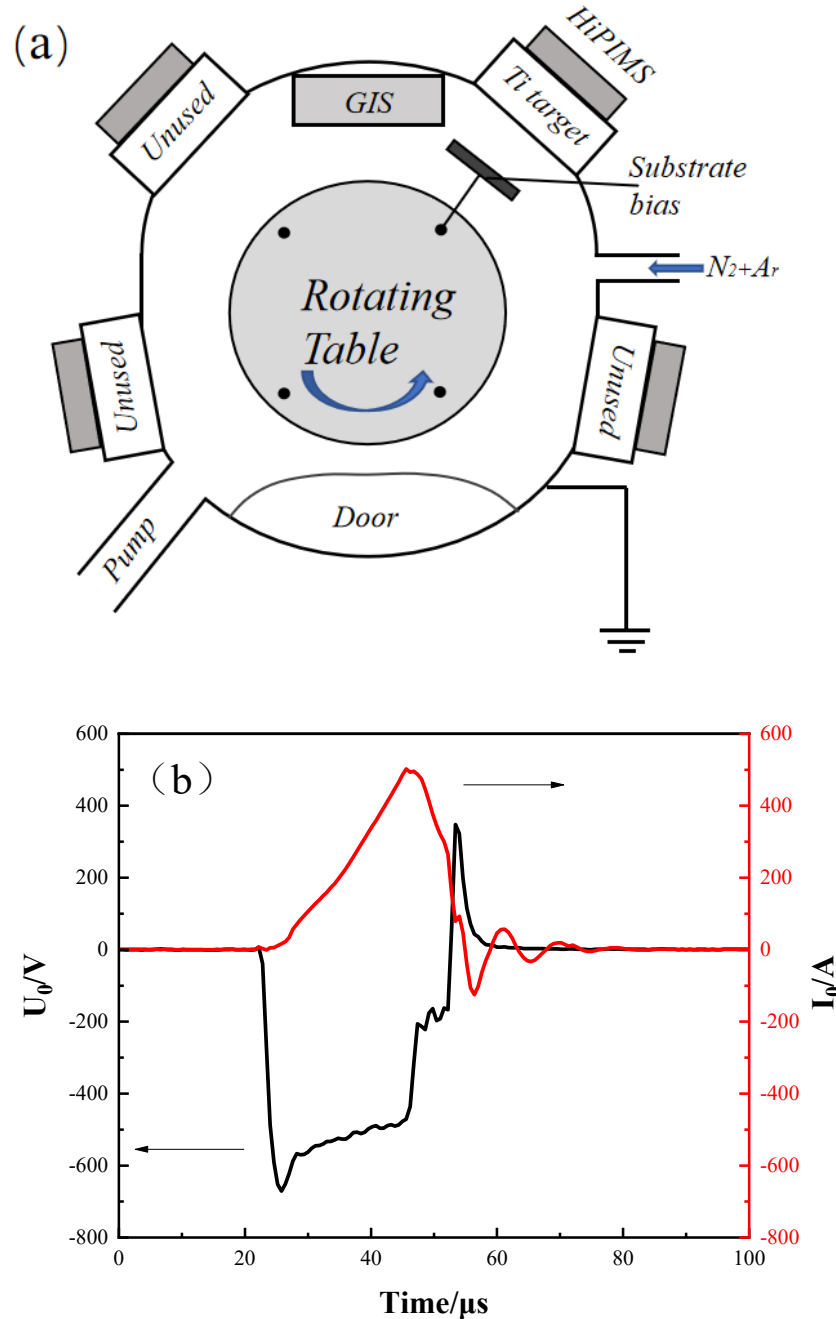


Figure 1. Schematic diagram of HiPIMS (a) and pulse shapes of the target current and voltage during coating depositions (b).

2.2. Morphology and Structure

The phase composition and crystal structure of the coatings were characterized using X-ray diffraction (XRD, X’Pert PRO MPD, PANalytical) (PANalytical, Almelo, The Netherlands) in a 0–2 θ configuration, with Cu K α radiation. The morphology of the films at various target powers was examined using an atomic force microscope (AFM, ToscaTM 400) (Anton Paar, Graz, Austria) in tapping mode. For observing the cross-sectional mor-

phologies of the coatings, field emission scanning electron microscopy (FESEM, Hitachi S-4800) (Hitachi, Tokyo, Japan) was utilized. Additionally, the compositional depth profiles of the coatings' cross sections were analyzed using a glow discharge optical emission spectrometer (GDA750HR, Spectrumba) (Spectrumba Analytik GmbH, Bayern, Germany).

2.3. Mechanical Properties and Adhesion

The hardness (H), elastic modulus (E), and elastic recovery (W_e) of the TiN coatings were measured using a nano-indenter (Nanoindenter XPTM, MTS Systems Corporation, Eden Prairie, MN, USA), equipped with a diamond indenter. To minimize the influence of the substrate, the indentation depth was consistently set to less than 10% of the total coating thickness. Coating–substrate adhesion was evaluated using a Rockwell hardness tester (HR-150A, HRA, MTS Systems Corporation, Eden Prairie, MN, USA) with an applied load of 1471 N (150 kg). The morphology of the indentations was examined using SEM to assess the adhesion level.

The fracture toughness was calculated using the length of radial cracks of Vickers indentations made using the microhardness tester (MMT-X, Matsuzawa, Okaya, Japan), under an applied load of 0.1 N. The fracture toughness, K_{IC} , of the coating was calculated using the following formula [18]: $K_{IC} = \alpha(E/H)^{1/2}(P/c^{3/2})$, where α is the empirical constant ($\alpha = 0.016$ for Vickers indenter). H, E, P and c are hardness, Young's modulus, applied max load, and the length of radial cracks, respectively. The depth of Vickers indentations is less than 10% of the coating thickness. Indentation tests were carried out six times in different regions of the film and the average values were calculated.

2.4. Wear Response and Endurance

The wear response and endurance of TiN coatings deposited at 6.5 kW were assessed using a reciprocating friction tribometer (MFT-5000, Huahui Instrument Technology Co., Ltd., Lanzhou, China), against a 6 mm diameter Si_3N_4 ball. Tests were conducted under normal loads ranging from 1 to 10 N. The sliding speed was maintained at 60 mm/s for a duration of 30 min, with the wear tracks measuring 5 mm in length. The morphology of the wear tracks was examined using FESEM, while the composition of the wear debris was analyzed using a Raman spectrometer. The specific wear rates were calculated using the following formula [19]: $k = V/LN$, where V is the wear volume of the wear track, N is the load, and L is the sliding distance.

Scratch testing of the coatings was performed using a micro-scratch tester (CSM Instrument, CSM Instruments, Peseux, Switzerland), with a progressive load from 0 to 30 N at a rate of 50 N/min over a scratch length of 3 mm. The wear tracks' profiles were measured with a surface morphology instrument (Talysurf 5P-120, Taylor Hobson, Leicester, UK). The abrasive debris and marks were further examined using a Raman spectrometer (HR-800, Jobin-Yvon, Jobin-HORIBA, Paris, France) equipped with an Ar-Kr laser at a wavelength of 532 nm. The spectrometer was used to scan in the range of 100–2000 cm^{-1} , to identify the composition and structural changes of the wear debris.

3. Results and Discussion

3.1. Surface Integrity and Microstructure

The phase structure of the coatings deposited using HiPIMS, with target powers ranging from 5 to 10 kW, were characterized using X-ray diffraction (XRD) analysis, as depicted in Figure 2a. These TiN coatings exhibited a monophasic face-centered cubic (fcc) structure. A notable shift in texture evolution from the (200) to the (111) orientation was observed with increasing target power. This shift in texture is intimately associated with the interplay between strain energy and surface energy within the fcc-structured TiN. Furthermore, this indicates a transition in the dominance from surface energy to strain energy [8]. The intensity indices of the (111) and (200) planes demonstrated inverse trends, varying within the ranges of 0.32–0.89 and 0.01–0.65, respectively, as shown in

Figure 2b. Additionally, diffraction peaks originating from the 304 stainless steel substrate were detected and are denoted as ‘SS’ in the XRD patterns.

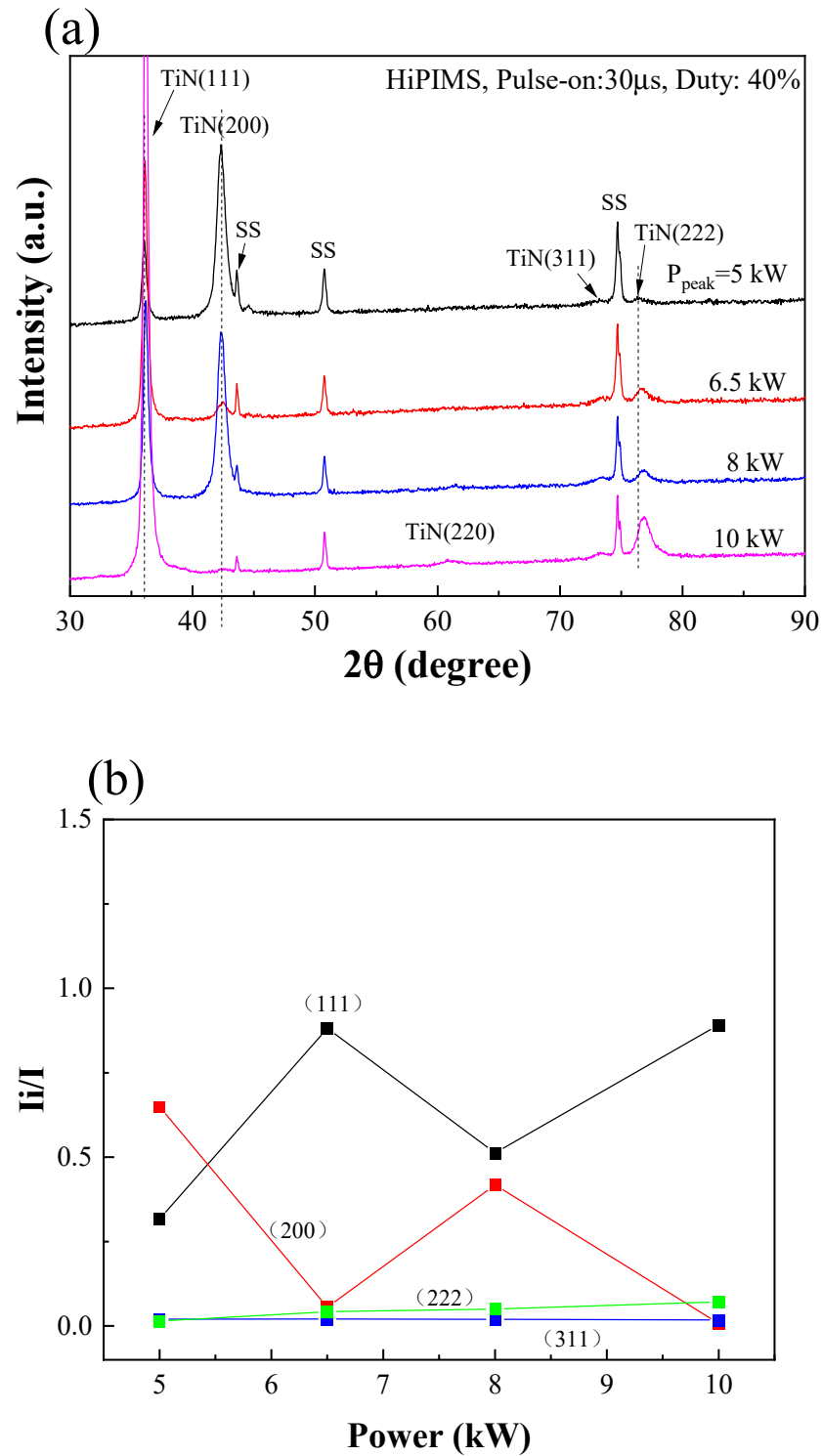


Figure 2. The XRD spectra of the HiPMS-sputtered TiN coatings (a) and the value of I_i/I (b) at 5–10 kW.

Surface integrity, including low surface roughness, a highly dense microstructure, and high uniformity, is essential for the mechanical and corrosion-resistant properties of coatings [20,21]. An atomic force microscope (AFM) was employed to examine the surface morphologies and surface roughness (Ra) of TiN coatings deposited at various

target powers, as illustrated in Figure 3a–d. The scanning area for AFM measurements is $1\ \mu\text{m} \times 1\ \mu\text{m}$, using tapping mode with a scanning speed of 70 nm/s. The coatings applied at 5 kW and 6.5 kW exhibited denser, smoother, and more uniform macrostructures. At 5 kW, a few large particles were observed on the coating surface. As the target power increased to 8 and 10 kW, numerous large particle clusters appeared on the surface, leading to a greater surface roughness compared to those deposited at 5 and 6.5 kW, as indicated in Figure 3e.

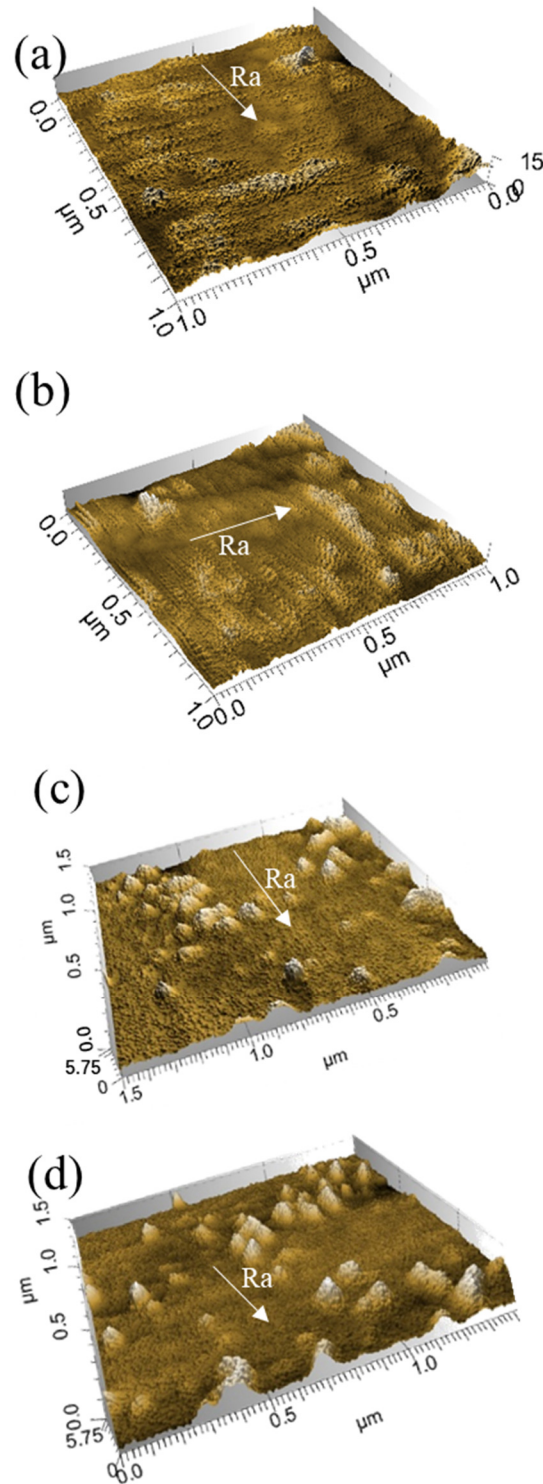


Figure 3. Cont.

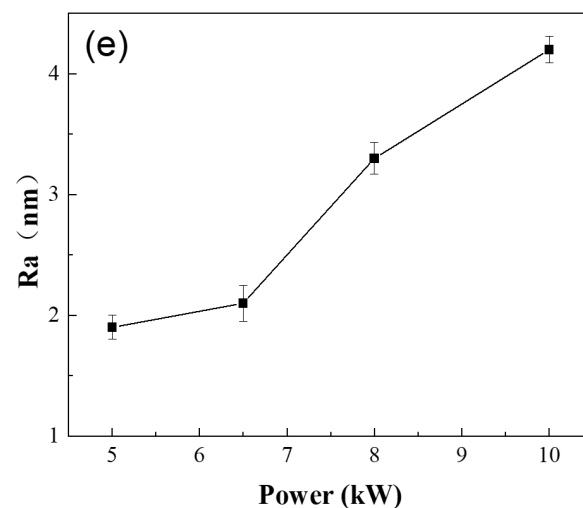


Figure 3. AFM images and surface roughness (Ra) of TiN coatings grown at various target powers: (a) 5 kW; (b) 6.5 kW; (c) 8 kW; (d) 10 kW; (e) Ra.

This increase in roughness can be attributed to the higher sputtering yield of target species atoms at elevated powers (8 and 10 kW), which generated a more substantial plasma ion flux and an enhanced ion bombardment onto the substrate, promoting grain growth. Additionally, the intense ion bombardment during film growth induced a re-sputtering effect, contributing to the increased surface roughness. Similar outcomes have been observed in other studies [20,22,23] conducted at higher sputtering powers, using HiPIMS.

Therefore, the coatings deposited at 5–6.5 kW demonstrated superior surface uniformity and density, which are anticipated to enhance the coatings' mechanical properties.

The cross-sectional FESEM images of the TiN coatings deposited at the various target powers are shown in Figure 4. The coatings are uniform and dense and the interfaces between coating and substrate are clear and sharp. All coatings maintain a similar thickness of about 1.6 μm . Figure 4e–h exhibit the GDOES composition depth of coatings with Ti and N elements in the coatings and Fe, Cr, and Ni elements contained in the 304 substrates. It can be seen that there are fewer Ti and N elements on the outer surface of the coating. Additionally, Ti is distributed uniformly in the inner part of the coating, while N is enriched in the coating. Both of these are beneficial for improving the hardness of the coatings. As reported by Y. Cheng [24], A. S. Mamaev [25], and E. Amzah [26], when N content increases within a certain range, the hardness and elastic modulus of TiN coating increases.

3.2. Mechanical Properties and Adhesion

Figure 5 illustrates the average values and distribution ranges of hardness (H), effective Young's modulus (E^*), H/E^* , and H^3/E^{*2} ratios for TiN coatings deposited using high-power impulse magnetron sputtering (HiPIMS) at varying target powers. As depicted in Figure 5a, there is a slight fluctuation in the average hardness as the target power changes. Initially, the hardness decreases from 31.3 GPa to 29.74 GPa with increasing target power, but then it increases again to 30.61 GPa. Despite these variations, all coatings maintain a high hardness level, averaging around 30 GPa, which indicates that they possess excellent elevated resistance to plastic deformation.

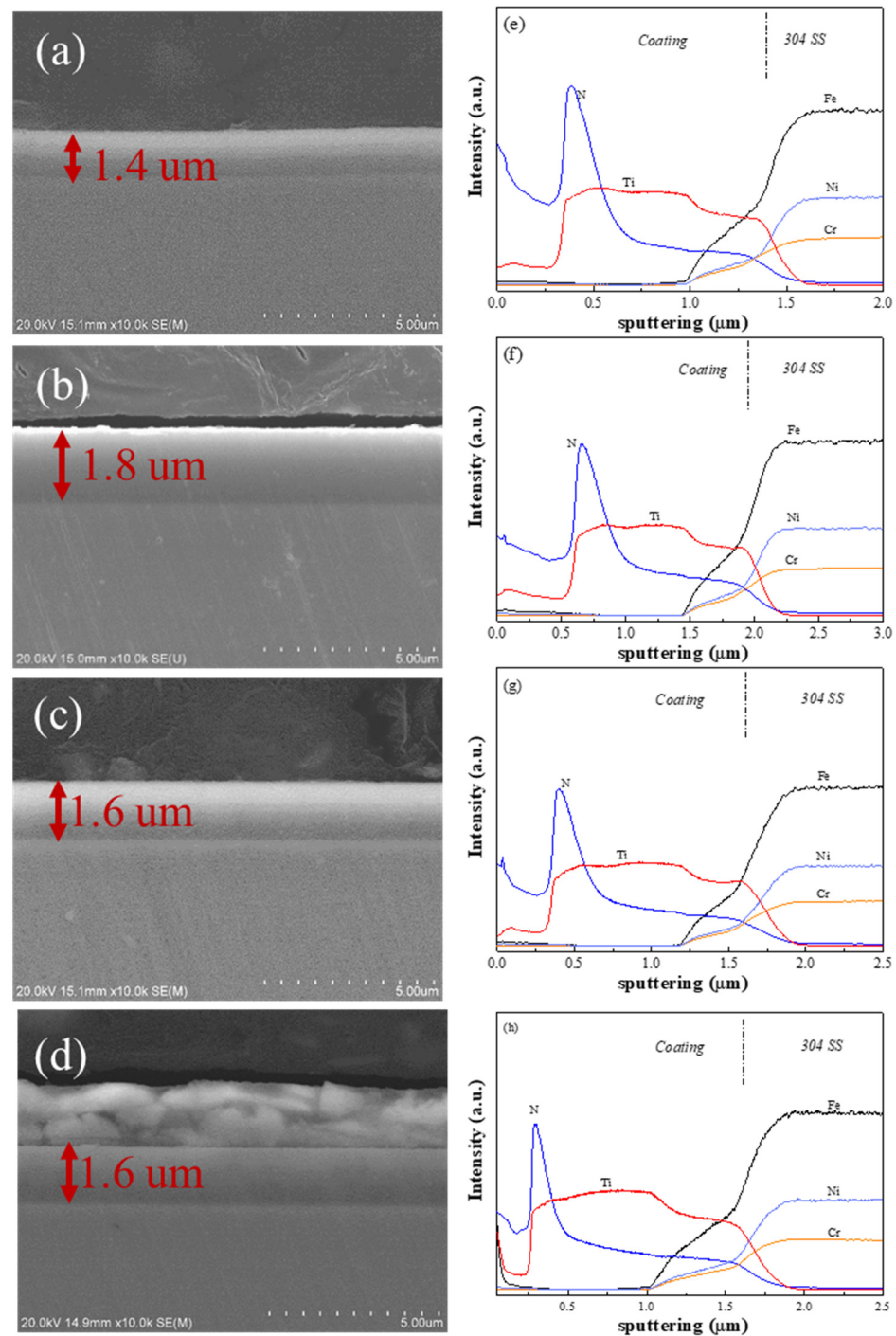


Figure 4. Cross-sectional SEM images and GDOES composition profiles of the TiN coatings deposited at different target powers. (a,e) 5 kW; (b,f) 6.5 kW; (c,g) 8 kW; (d,h) 10 kW.

The increased toughness of hard ceramic coatings, such as TiN, is known to improve friction and wear performance. This improvement is attributed to the coatings' enhanced resistance to cracking, which is a result of their surface integrity and distinctive nanostructure [11,12]. The H/E^* and H^3/E^{*2} ratios are dimensionless parameters often used to assess the wear resistance of materials; higher values typically suggest better wear performance. These ratios follow a similar trend to that of the Young's modulus and hardness. They increase from 0.093 and 0.270 at 5 kW to their maximum values of 0.097 and 0.290, respectively, at a target power of 6.5 kW. However, they then decrease to 0.084 and 0.215 at a target power of 10 kW.

The peak values of these ratios at 6.5 kW suggest that, at this particular target power, the coatings have an optimal balance of hardness and elasticity, which is conducive to better wear resistance. The subsequent decrease in these ratios at higher powers indicates a relative reduction in this balance, which could potentially lead to a diminished wear performance.

The micro-indentation images included in Figure 5c provide additional insights into the mechanical properties of the TiN coatings, particularly their fracture toughness. Under a load of 0.1 N, the absence of radial cracks around the Vickers indentations suggests that the coatings have excellent fracture toughness, which is a critical property for the durability and longevity of coatings in practical applications.

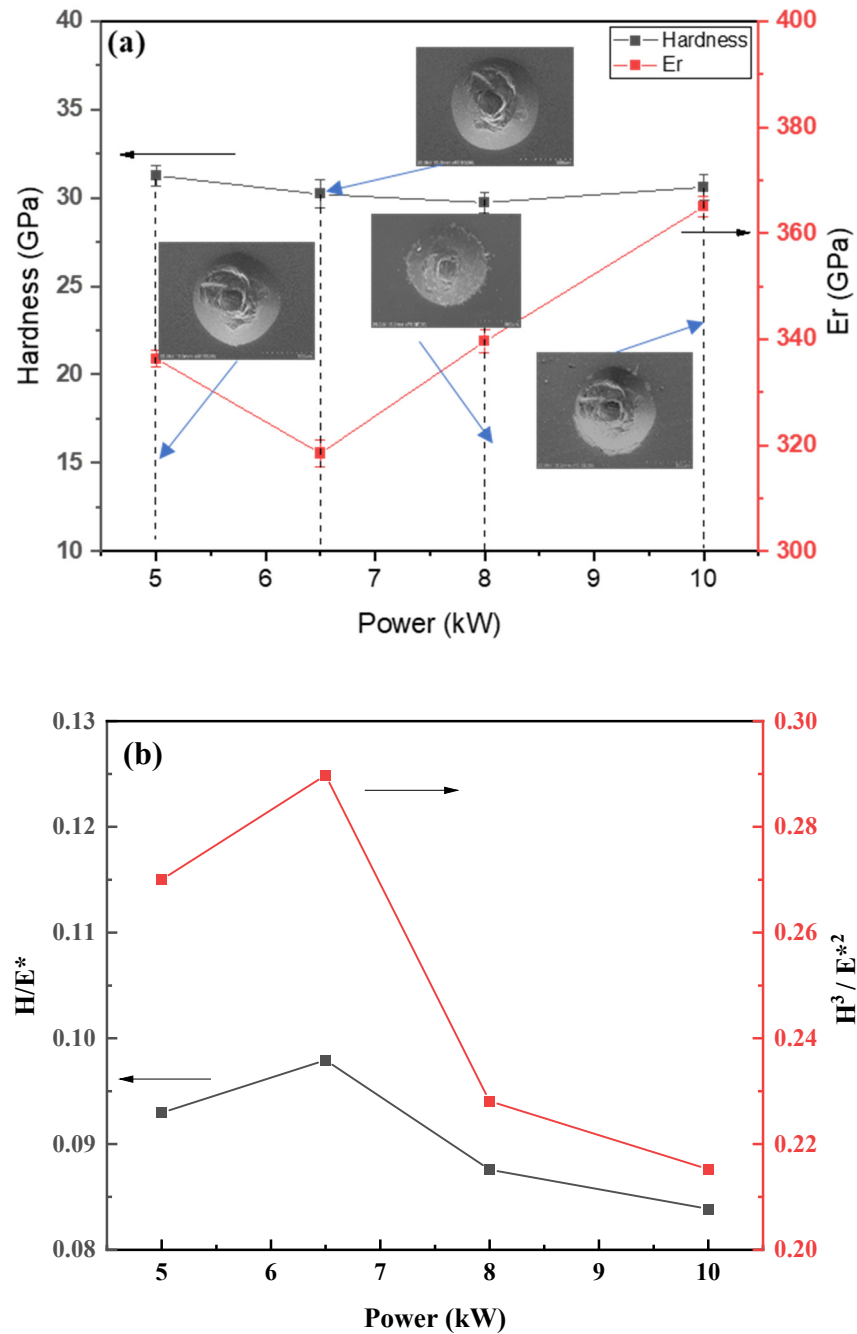


Figure 5. Cont.

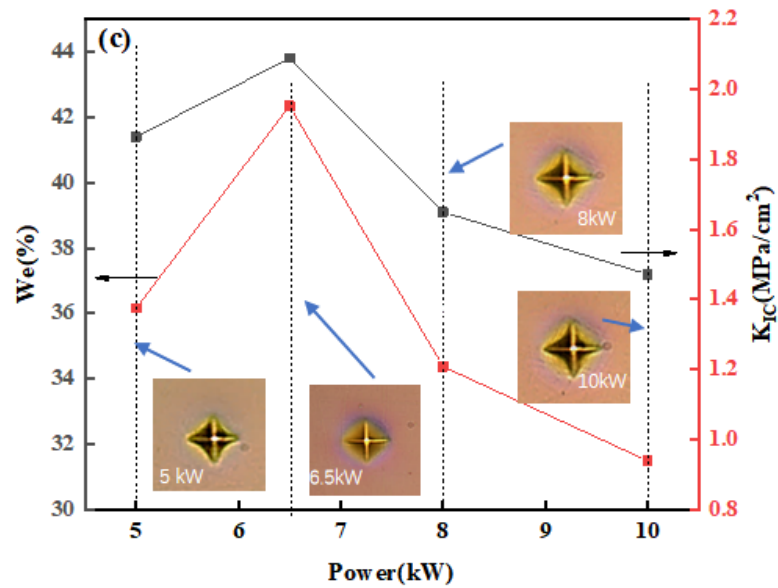


Figure 5. (a) Hardness (H), effective Young’s modulus (E*), and the Micro-Vickers indentations inserted in; (b) H/E* and H³/E*² ratios of TiN coatings deposited using HiPIMS at various target powers; (c) We, K_{1C}, and the Micro-Vickers indentations inserted.

At a HiPIMS power of 6.5 kW, the coatings exhibit smooth and smaller indentations, which is indicative of a higher fracture toughness. Achieving a combination of high hardness and high toughness in coatings is challenging, because these properties are often mutually exclusive [27]. However, highly ionized reactive sputtering techniques, such as reactive HiPIMS and deep oscillation magnetron sputtering, can achieve this balance [20,28].

The coatings prepared in this study demonstrate both high hardness and excellent toughness, particularly at 6.5 kW. This is likely due to the dense nanostructure and finely refined grains of the coatings. At the lower target power of 5 kW, the sputtering power is insufficient, resulting in low Ti atomic activity and film forming efficiency. As the target power increases to 6.5 kW, the supply of atoms necessary for the growth of the TiN coating is optimized, leading to good film–substrate adhesion and film density (see Figures 3 and 6). However, further increasing the target power to 8 kW and 10 kW increases the tensile stress within the coating, due to the higher energy and number of sputtered atoms, which reduces the fracture toughness [29].

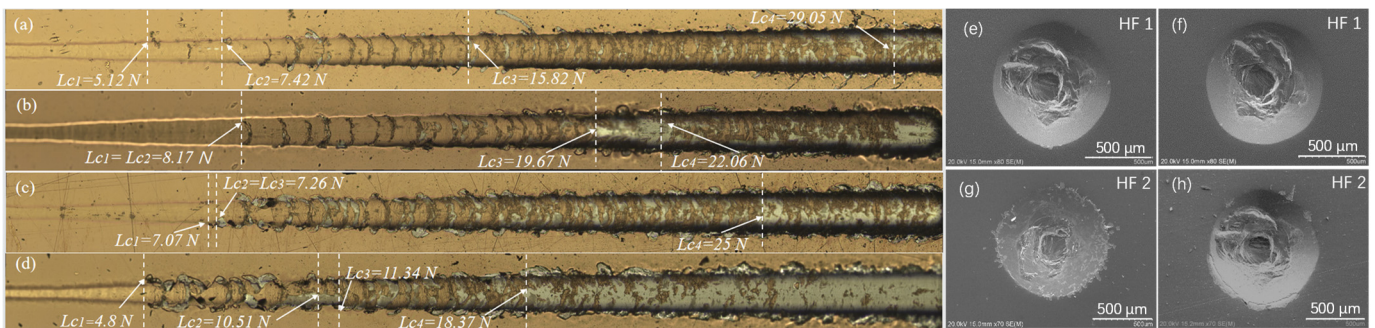


Figure 6. Typical scratch morphology of TiN coatings deposited at various target powers (a) 5 kW; (b) 6.5 kW; (c) 8 kW; (d) 10 kW.

The difference in performance between hard coatings and soft substrates is significant, especially in response to cooperative deformation during cracking [12]. Therefore, in the design of hard coating/substrate systems, it is crucial to prevent or delay the initiation and

propagation of cracks to improve the cooperative deformation between the hard coating and the soft substrate [30].

The fracture behavior of the TiN hard coatings is evaluated using Vickers indentation tests in combination with calculated fracture toughness values. Figure 5c shows the W_e and K_{IC} values. The optical micrographs of the Vickers micro-indentations indicate that the radial crack length first increases and then decreases, with the K_{IC} value peaking at 6.5 kW. This peak corresponds to the best fracture toughness of the coating. As the target power increases to 8 kW and 10 kW, the tensile stress and, consequently, the fracture toughness decrease. The W_e and K_{IC} values follow a similar trend with increasing target power, reaching their maximum at 6.5 kW, due to the highest H/E^* and H^3/E^{*2} ratios, which suggest high strength and resistance to crack formation and propagation under local dynamic loads [12,14]. Therefore, the coatings deposited at 6.5 kW present an optimal balance of hardness and toughness, making them highly resistant to wear and fracture.

The adhesion and cohesion of coatings are an important index to judge the quality of hard coatings. The cohesion and adhesion level of TiN coatings deposited at various target powers were evaluated using micro-scratch and Rockwell C tests. The optical morphologies of scratch tracks and SEM images of HRC indents of TiN coatings are shown in Figure 6. As Ti target power increased from 5 to 6.5 kW, L_{C1} , L_{C2} , and L_{C3} varied from 5.12 N to 8.17 N, 5.12 N to 8.17 N, and 7.26 N and 19.67 N, respectively. The critical load (L_{C1} , L_{C2} , and L_{C3}) showed a maximum value at 6.5 kW. Meanwhile, the coherent transition from plastic deformation to fracture in the scratch track indicates an enhanced cooperative deformation between the coating and the substrate system. The coating was completely peeled off and the substrate was exposed when the load was higher than 18.37 N at 10 kW, indicating that the coating has a poor binding force at this deposited power. The critical loads showed a similar tendency as those of the H/E^* and H^3/E^{*2} ratios. The increased critical loads benefited from the combined effect of the increased H/E^* and H^3/E^{*2} ratios.

According to VDI 3198 rules [31], the criteria of each level (HF1-HF4) is determined according to the damage of the coating adjacent to the indentation boundary of hard ceramic coatings. In general, the radial cracks are caused by the plastic deformation of the substrate and the weak adhesion of substrate/coating interfaces [32]. In this work, there are few radial cracks along the indentation in the coatings prepared, indicating that the coatings have a high fracture toughness. Figure 6e–h present the SEM images with an applied load of 150 kg of TiN coatings deposited at different target powers. According to Heinke [33], the coatings showed an improved adhesion level of above HF1 with no delamination or cracks in the indentation of the sample at 5 and 6.5 kW, as shown in Figure 6e,f. The increase in the target power radial cracks can be observed at 8 kW and part of the coating edge fell off at 10 kW; the adhesion strength was assessed as HF2 at 8 kW and 10 kW. The enhancement of coating adhesion and cohesion is mainly determined by the increase in coating H , H/E^* , and H^3/E^{*2} [29]. The increase in adhesion and cohesion indicates the improved cooperative deformation between coating and softer matrix [34].

3.3. Tribological Behaviors

Based on the evaluation results, TiN coatings deposited at 6.5 kW exhibit high hardness, excellent adhesion, and superior toughness. Additionally, they enable effective cooperative deformation between the coating and the substrate under the same deposition conditions, which is advantageous for reducing friction and wear [14,15,21]. However, as the target power increases to 10 kW, the mechanical properties of the coating generally decline. Consequently, we investigated the tribological and wear characteristics of the coatings under normal loads of up to 10 N, to assess the durability of the coatings applied at 6.5 kW. Figure 7a displays the friction coefficient (COF) of TiN coatings deposited at 6.5 kW against Si_3N_4 balls under loads ranging from 1 to 10 N.

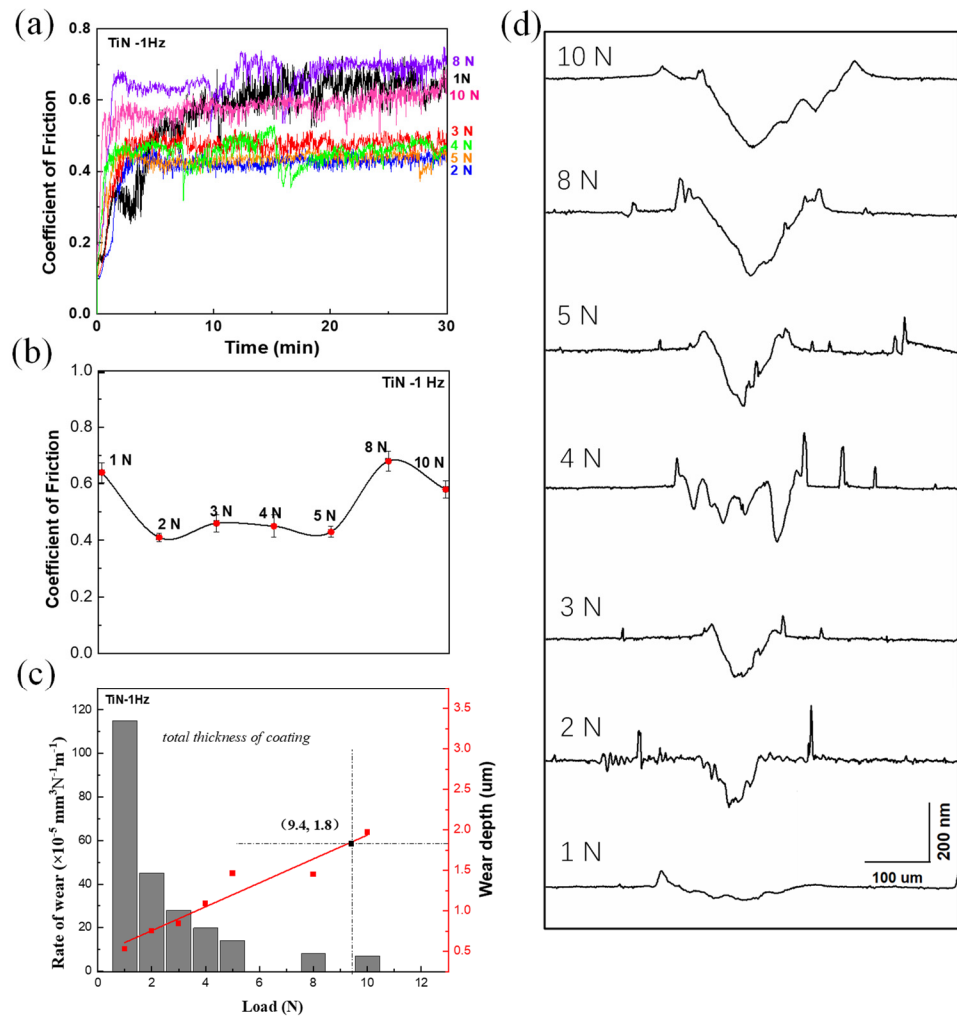


Figure 7. Friction coefficient as a function of time (a); the COF value (b); wear rate and wear depth (c); and the profile of wear trace (d).

After a prolonged period of 12 min under a 1 N load, the COF sharply rose to 0.6 and exhibited oscillatory behavior. The FESEM images of the worn surfaces, as shown in Figure 8a–h, reveal that the coatings underwent oxidative wear, characterized by the presence of flake-like and fine oxide films along the wear track. At applied loads of 2–5 N, the COF rapidly stabilized at 0.4, which is indicative of a shorter run-in period compared to the 1 N load. The coatings experienced a combination of oxidative and abrasive wear, with fine oxides and a slight material transfer observed within and along the wear track edges.

Under an 8 N load, pronounced grooves and fine abrasive particles were detected within and beside the wear track, leading to COF fluctuations. At this load, the primary wear mechanism was intense abrasive wear. Increasing the sliding load to 10 N resulted in deeper grooves within the wear track and reduced COF oscillation compared to the 8 N load. As indicated by the wear profile in Figure 7d and the wear depth in Figure 7c, the wear depth remained below the TiN coating thickness for loads up to 8 N. However, at a 10 N load, the wear depth reached 1.97 μm , surpassing the coating thickness of 1.8 μm . This suggests that the TiN coating was completely worn through and the Si_3N_4 ball was in direct contact with the 304 substrate, causing only slight fluctuations in the friction coefficient. The wear mechanism at this stage is predominantly severe abrasive wear.

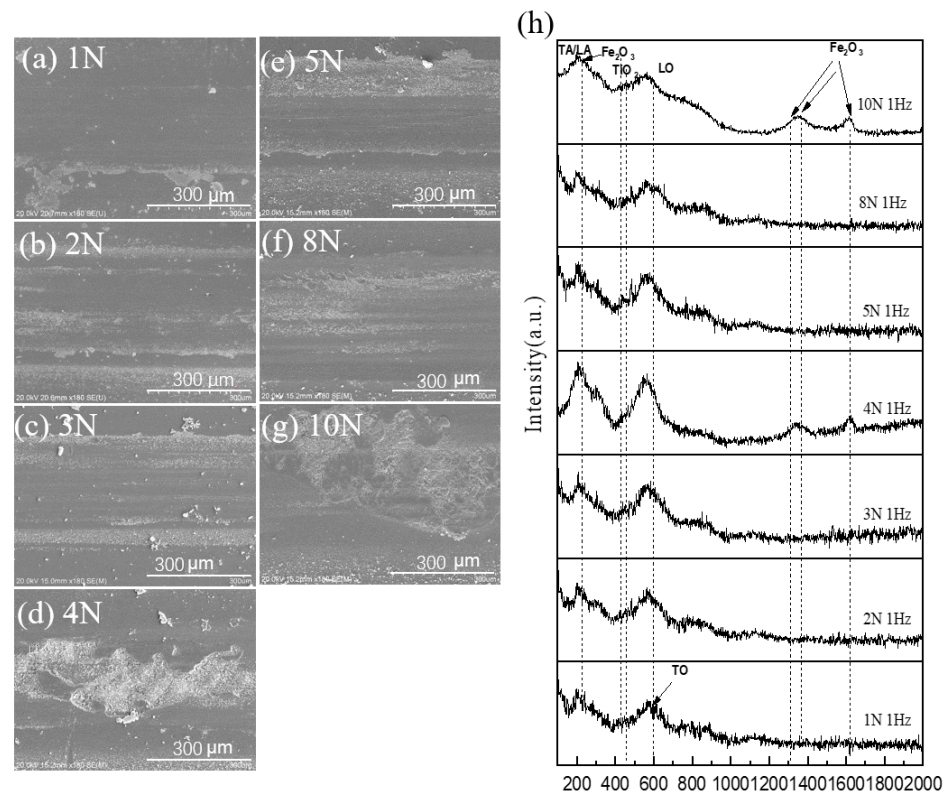


Figure 8. The morphology (a–g) and the Raman diagram (h) of wear trace with the normal load of 1–10 N.

Figure 7c illustrates that both the width and depth of the wear track increase with the normal load and this trend is seen almost throughout the entire scratch track. Figure 7b indicates that, at loads of 2–5 N, the coating maintained a stable wear equilibrium, with the COF consistently around 0.43. This stability can be attributed to the high H/E^* and H^3/E^{*2} ratios of the TiN coating deposited at 6.5 kW, which confer their hard yet tough properties. The wear resistance of the TiN coating, which is both hard and tough, has an optimal load-bearing range of 2–5 N, as shown in Figure 7b, where the wear process stabilizes, significantly enhancing the coating's wear resistance and expanding its application potential.

According to the Raman spectroscopy results presented in Figure 8h, TiO_2 was detected in the wear tracks under all tested loads, likely due to the oxidation of the wear debris during the wear process. Additionally, Fe_2O_3 was identified at a 10 N load, with iron originating from the 304 substrate, further confirming that the TiN coating was breached at this load.

4. Conclusions

- (1) Hard yet tough TiN coatings with single-phase face-centered cubic structures were deposited using high-power impulse magnetron sputtering at a target power of 5–10 kW. As the target power increased, TiN coatings showed a texture evolution from (200) to (111). The hardness (H) had a slight fluctuation of 29.8–31.2 GPa, while the effective Young's modulus (E^*) was 310–365 GPa. The H/E^* and H^3/E^{*2} ratios are 0.083–0.1 and 0.215–0.29, respectively, with increasing target power. The coatings possessed a favorable toughness, without radial cracks forming in micro-indentations, as well as a uniform failure before critical failure load, due to the increased H/E^* and H^3/E^{*2} ratios attributed to surface integrity and texture evolution. The TiN coatings prepared at 5 kW exhibit stable friction coefficients and wear behavior under loads of 2–5 N, compared to those of the TiN coatings reported in the literature. The TiN

coatings prepared at 5 kW in this work exhibit stable friction coefficients and wear behavior under loads of 2–5 N, while they often demonstrate different tribological behaviors under varying loads, when reported in the literature.

- (2) The wear response of hard yet tough TiN coatings was investigated under loads of 1–10 N. With an increase in sliding load, the wear mechanism changed from oxidative wear at the normal load of 1 N to severe abrasive wear at 10 N. At a load of between 2 and 5 N, the coatings suffer from a mixture of oxidative and abrasive wear. The endurance of the coatings is regarded as the load of 9.4 N and the depth of wear track at 1.8 μm .

Author Contributions: Conceptualization, Q.Z.; Methodology, Y.O. and W.X.; Software, Q.Z., F.L., Y.X. and G.Q.; Validation, Q.H.; Formal analysis, Q.Z.; Resources, B.L.; Data curation, J.C.; Writing—original draft, Q.Z.; Writing—review & editing, Y.O.; Visualization, C.O.; Supervision, C.O. All authors have read and agreed to the published version of the manuscript.

Funding: This work was supported by the National Natural Science Foundation of China (Grant No. 12275028), the 2024 innovation projects from Beijing Academy of Science and Technology, the Guangdong Province Key Area Research and Development Program (Grant No. 2019B090909002), and the National Key R&D Program of China (2023YFB4005901).

Institutional Review Board Statement: Not applicable.

Informed Consent Statement: Not applicable.

Data Availability Statement: The raw/processed data required to reproduce these findings cannot be shared at this time, as the data also forms part of an ongoing study.

Conflicts of Interest: Feiqiang Li, Yunfei Xu, Jidong Cao and Guanshu Qu were employed by the company Beijing SinoHytec Co., Ltd. The remaining authors declare that the research was conducted in the absence of any commercial or financial relationships that could be construed as a potential conflict of interest.

References

1. Sundgren, J.-E. Structure and properties of TiN coatings. *Thin Solid Film*. **1985**, *128*, 21–44. [[CrossRef](#)]
2. Chou, W.J.; Yu, G.P.; Huang, J.H. Mechanical properties of TiN thin film coatings on 304 stainless steel substrates. *Surf. Coat. Technol.* **2002**, *149*, 7–13. [[CrossRef](#)]
3. Rebenne, H.E.; Bhat, D.G. Review of CVD TiN coatings for wear-resistant applications: Deposition processes, properties and performance. *Surf. Coat. Technol.* **1994**, *63*, 1–13. [[CrossRef](#)]
4. Ou, Y.X.; Wang, H.Q.; Ouyang, X.; Zhao, Y.Y.; Zhou, Q.; Luo, C.W.; Hua, Q.S.; Ouyang, X.P.; Zhang, S. Recent advances and strategies for high-performance coatings. *Prog. Mater. Sci.* **2023**, *136*, 101125. [[CrossRef](#)]
5. Wang, X.Z.; Ye, C.P.; Shi, D.D.; Fan, H.Q.; Li, Q. Potential polarization accelerated degradation of interfacial electrical conductivity for Au/TiN coated 316L SS bipolar plates used in polymer electrolyte membrane fuel cells. *Corros. Sci.* **2021**, *189*, 109624. [[CrossRef](#)]
6. Wang, Y.X.; Zhang, S. Toward hard yet tough ceramic coatings. *Surf. Coat. Technol.* **2014**, *258*, 1–16. [[CrossRef](#)]
7. Nordin, M.; Larsson, M. Deposition and characterisation of multilayered PVD TiN/CrN coatings on cemented carbide. *Surf. Coat. Technol.* **1999**, *116–119*, 108–115. [[CrossRef](#)]
8. Escalona, M.; Bhuyan, H.; Ibacache, S.; Retamal, M.J.; Saikia, P.; Borgohain, C.; Valenzuela, J.C.; Veloso, F.; Favre, M.; Wyndham, E. Study of titanium nitride film growth by plasma enhanced pulsed laser deposition at different experimental conditions. *Surf. Coat. Technol.* **2021**, *405*, 126492. [[CrossRef](#)]
9. Hong, X.; Feng, K.; Tan, Y.; Wang, X.L.; Tan, H. Effects of process parameters on microstructure and wear resistance of TiN coatings deposited on TC11 titanium alloy by electrospark deposition. *Trans. Nonferrous Met. Soc. China* **2017**, *27*, 1767–1776. [[CrossRef](#)]
10. Wang, Y.X.; Zhang, S.; Lee, J.-W. Hard Yet Tough Ceramic Coating: Not a Dream Any More—I. via Nanostructured Multilayering. *Nanosci. Nanotechnol. Lett.* **2012**, *4*, 375–377. [[CrossRef](#)]
11. Wang, Z.Y.; Li, X.W.; Wang, X.; Sheng, C.; Ke, P.L.; Wang, A.Y. Hard yet tough V-Al-C-N nanocomposite coatings: Microstructure, mechanical and tribological properties. *Surf. Coat. Technol.* **2016**, *304*, 553–559. [[CrossRef](#)]
12. Ou, Y.X.; Ouyang, X.P.; Liao, B.; Zhang, X.; Zhang, S. Hard yet tough CrN/Si₃N₄ multilayer coatings deposited by the combined deep oscillation magnetron sputtering and pulsed dc magnetron sputtering. *Appl. Surf. Sci.* **2020**, *502*, 144168. [[CrossRef](#)]
13. Hogmark, S.; Hedenqvist, P. Tribological characterization of thin, hard coatings. *Wear* **1994**, *179*, 147–154. [[CrossRef](#)]
14. Jiang, D.Y. Recent progresses in the phenomenological description for the indentation size effect in microhardness testing of brittle ceramics. *J. Adv. Ceram.* **2012**, *1*. [[CrossRef](#)]

15. Chen, Q.; Cao, Y.Z.; Xie, Z.W.; Chen, T.; Wan, Y.Y.; Wang, H.; Gao, X.; Chen, Y.; Zhou, Y.W.; Guo, Y.Y. Tribocorrosion behaviors of CrN coating in 3.5 wt.% NaCl solution. *Thin Solid Film*. **2017**, *622*, 41–47. [[CrossRef](#)]
16. Zhang, S.; Sun, D.; Fu, Y.Q.; Du, H.J. Toughness measurement of thin films: A critical review. *Surf. Coat. Technol.* **2005**, *198*, 74–84. [[CrossRef](#)]
17. Philippon, D.; Godinho, V.; Nagy, P.M.; Delplancke-Ogletree, M.P.; Fernández, A. Endurance of TiAlSiN coatings: Effect of Si and bias on wear and adhesion. *Wear* **2011**, *270*, 541–549. [[CrossRef](#)]
18. Marshall, D.B.; Lawn, B.R.; Evans, A.G. Elastic/plastic indentation damage in ceramics: The lateral crack system. *J. Am. Ceram. Soc.* **1982**, *65*, 561–566. [[CrossRef](#)]
19. An, D.; Choi, J.H.; Schmitz, T.L.; Kim, N.H. In situ monitoring and prediction of progressive joint wear using Bayesian statistics. *Wear* **2011**, *270*, 828–838. [[CrossRef](#)]
20. Ou, Y.X.; Wang, H.Q.; Hua, Q.S.; Liao, B.; Ouyang, X.P. Tribocorrosion behaviors of superhard yet tough Ti-C-N ceramic coatings. *Surf. Coat. Technol.* **2022**, *439*, 128448. [[CrossRef](#)]
21. Grilli, M.L.; Valerini, D.; Slobozeanu, A.E.; Postolnyi, B.O.; Balos, S.; Rizzo, A.; Piticescu, R.R. Critical raw materials saving by protective coatings under extreme conditions: A review of last trends in alloys and coatings for aerospace engine applications. *Materials* **2021**, *14*, 1656. [[CrossRef](#)] [[PubMed](#)]
22. Quillin, K.; Yeom, H.; Dabney, T.; McFarland, M.; Sridharan, K. Experimental evaluation of direct current magnetron sputtered and high-power impulse magnetron sputtered Cr coatings on SiC for light water reactor applications. *Thin Solid Film*. **2020**, *716*, 138431. [[CrossRef](#)]
23. Zhang, R. *Diamond Based Materials and Nanostructures for Advanced Functional Applications*; University of Leicester: Leicester, UK, 2024.
24. Cheng, Y.; Zheng, Y.F. Effect of N₂/Ar gas flow ratio on the deposition of TiN/Ti coatings on NiTi shape memory alloy by PIIID. *Mater. Lett.* **2006**, *60*, 2243–2247. [[CrossRef](#)]
25. Mamaev, A.S.; Chukin, A.V. Effect of the nitrogen flow rate on the microhardness and microstructure of TiN coatings deposited by high power pulsed magnetron sputtering. Surface investigation, X-ray. *Synchrotron Neutron Tech.* **2015**, *9*, 980–983. [[CrossRef](#)]
26. Hamzah, E.; Ourdjini, A. Influence of nitrogen flow rate on friction coefficient and surface roughness of TiN coatings deposited on tool steel using arc method. *Surf. Rev. Lett.* **2007**, *14*, 1007–1013. [[CrossRef](#)]
27. Zhang, S.; Wang, H.L.; Ong, S.E.; Sun, D.; Bui, X.L. Hard yet tough nanocomposite coatings present status and future trends. *Plasma Process. Polym.* **2007**, *4*, 219. [[CrossRef](#)]
28. Jiang, Z.T.; Lei, M.K. Structure and fracture toughness of TiAlN thin films deposited by deep oscillation magnetron sputtering. *Thin Solid Film*. **2022**, *754*, 139306. [[CrossRef](#)]
29. Hu, J.; Li, H.; Li, J.; Yan, C.; Kong, J.; Wu, Q.; Xiong, D. Super-hard and tough Ta_{1-x}W_xCy films deposited by magnetron sputtering. *Surf. Coat. Technol.* **2020**, *400*, 126207. [[CrossRef](#)]
30. Tian, L.H.; Zhu, R.H.; Yao, X.H.; Yang, Y.J. Fracture behavior of CrN coatings under indentation and dynamic cycle impact. *J. Wuhan Univ. Technol.* **2012**, *27*, 4. [[CrossRef](#)]
31. Verein Deutscher Ingenieure Normen. *VDI 3198*; VDI Verlag: Düsseldorf, Germany, 1991.
32. Rezakhanlou, R.; Stebut, J.V. Damage Mechanisms of Hard Coatings on Hard Substrates: A Critical Analysis of Failure in Scratch and Wear Testing. *Tribol. Ser.* **1990**, *17*, 183–192.
33. Heinke, W.; Leyland, A.; Matthews, A.; Berg, G.; Friedrich, C.; Broszeit, E. Evaluation of PVD nitride coatings, using impact, scratch and Rockwell-C adhesion tests. *Thin Solid Film*. **1995**, *270*, 431–438. [[CrossRef](#)]
34. Dalibón, E.L.; Escalada, L.; Simison, S.; Forsich, C.; Heim, D.; Brühl, S.P. Mechanical and corrosion behavior of thick and soft DLC coatings. *Surf. Coat. Technol.* **2017**, *312*, 101–109. [[CrossRef](#)]

Disclaimer/Publisher's Note: The statements, opinions and data contained in all publications are solely those of the individual author(s) and contributor(s) and not of MDPI and/or the editor(s). MDPI and/or the editor(s) disclaim responsibility for any injury to people or property resulting from any ideas, methods, instructions or products referred to in the content.